

THE SPECIFIC DYNAMIC CAPACITY OF A PLANETARY ROLLER SCREW WITH RANDOM DEVIATIONS OF THE THREAD PITCH

FILIP LISOWSKI

Cracow University of Technology, Institute of Machine Design, Cracow, Poland

e-mail: ftisow@mech.pk.edu.pl

The paper presents an analysis of the specific dynamic capacity of a planetary roller screw including random deviations of the thread pitch. Results are based on a statistical analysis of loads between the screw and the roller obtained for the accepted bar model to determine the load distribution. Furthermore, the finite element analysis has been applied to determine stiffness coefficients of the screw-roller and the roller-nut cooperation. The purpose of the following considerations is to assess a decrease in the specific dynamic capacity of the planetary roller screw depending on random deviations of the thread pitch.

Key words: planetary roller screw, specific dynamic capacity, random deviations

1. Introduction

The planetary roller screw (PRS) is a highly efficient mechanical actuator for demanding applications (Fig. 1). The mechanism is used to convert rotational motion into linear motion or in the other way round. The main advantage of PRS is very high load capacity while maintaining high speed of operation and high positioning accuracy.

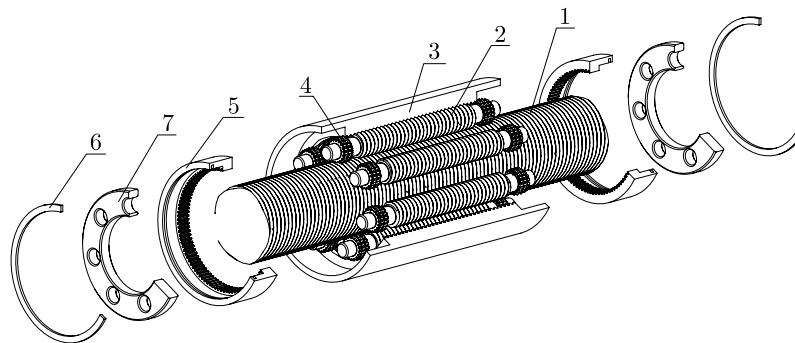


Fig. 1. Structure of the planetary roller screw (exploded view); 1 – screw, 2 – roller, 3 – nut, 4 – satellite gear, 5 – ring gear, 6 – retainer ring, 7 – annular hoop

One of the major problems concerning planetary roller screws is the carrying capacity related to the load distribution between cooperating elements. Theoretical load characteristics provide information about the most loaded regions of threads and enable determination of the equivalent load. Several authors of previous publications related to the planetary roller screw considered models for determination of the load distribution. Ma *et al.* (2012) adopted a model developed for ball screws given by Xuesong *et al.* (2003) to determine the static load distribution. The rollers were assumed as rigid bodies and only contact deformations of threads were involved in calculations based on the Hertzian theory. Ryś and Lisowski (2014) presented an analytical model for determination of the load distribution between cooperating elements for an arbitrary number of rollers. The idea of the model was to consider deformations of engaged elements as

deformations of rectangular volumes subjected to shear stresses. Contact deformations of threads and deformations of the screw and nut cores were taken into account by a properly chosen shear modulus. However, the model was intended only for the preliminary design. Lisowski (2014) proposed a model to determine the load distribution between the roller and the screw as well as between the roller and the nut, which allowed one to take into account contact deformations of threads and deformations of the screw and nut cores. Also, the various thread profiles were considered.

Lastly, Jones and Velinsky (2014) used the direct stiffness method to construct a model which considered the roller screw mechanism as a large spring system composed of individual springs referred to various elements. The authors used their method to calculate the axial stiffness of PRS and the load distribution between particular elements. In an earlier article, Velinsky *et al.* (2009) analysed kinematics, efficiency and the load carrying capacity. The load carrying capacity was derived based on geometric conditions and equilibrium of forces.

Recently, Abevi *et al.* (2015) presented a method to compute the static load distribution in any type of planetary roller screw based on a hybrid model including one-dimensional finite elements and non-linear springs.

However, apart from theoretical load distributions determined for nominal dimensions of cooperating threads, it is also essential to take into account the impact of manufacturing deviations. Deviations of the thread pitch affect theoretical load distributions between cooperating elements and, therefore, they impact the specific dynamic capacity of the planetary roller screw.

Although some authors have mentioned the importance of the impact of random deviations on the load distribution, the problem related to PRS has not been analysed in publications yet. In turn, a similar problem but related to helical gears was analysed by Ryś (1990). The author studied the impact of random deviations of the gears pitch on static and dynamic loads. Owing to dynamic overload, mostly the problem of start-up was analysed.

This paper presents an analysis of the impact of random deviations of the thread pitch on the specific dynamic capacity of the planetary roller screw mechanism. The results are based on a statistical analysis of the loads on threads, obtained based on the bar model.

2. The load distribution between cooperating elements – bar model

In order to determine the load distribution between cooperating elements of the planetary roller screw, a bar model proposed by Lisowski (2014), has been accepted. This model is preferable as it enables taking into account random deviations of the thread pitch for particular pairs of threads. However, determining the stiffness of a single pair of cooperating threads of the screw and the roller as well as the roller and the nut requires doing an additional finite element analysis.

The model refers to the section of PRS including one roller cooperating with the screw and the nut as shown in Fig. 2. The number of cooperating threads is arbitrary. Also, various thread profiles can be accepted by assuming proper stiffness parameters obtained from FEA.

For further considerations, the following assumptions have been made: the core of the roller is non-deformable; cores of the screw and the nut are deformable; threads of the roller, screw and the nut are deformable; stiffness of the screw core is close to stiffness of the nut core; forces in the screw and nut cores change in steps. Due to the small helix angle, the forces q_{s_j} and q_{n_j} belong to the same plane; the external force Q is distributed proportionally into the rollers.

The axial forces in the screw and nut cores can be consistent or opposite. The system of forces shown in Fig. 2 which refers to the case when both the screw and the nut are compressed (a) or the screw is compressed while the nut is tensioned (b). However, depending on locations where the forces are applied, it is also possible to obtain two other cases in which both the screw and the nut are tensioned or the screw is tensioned while the nut is compressed. In further

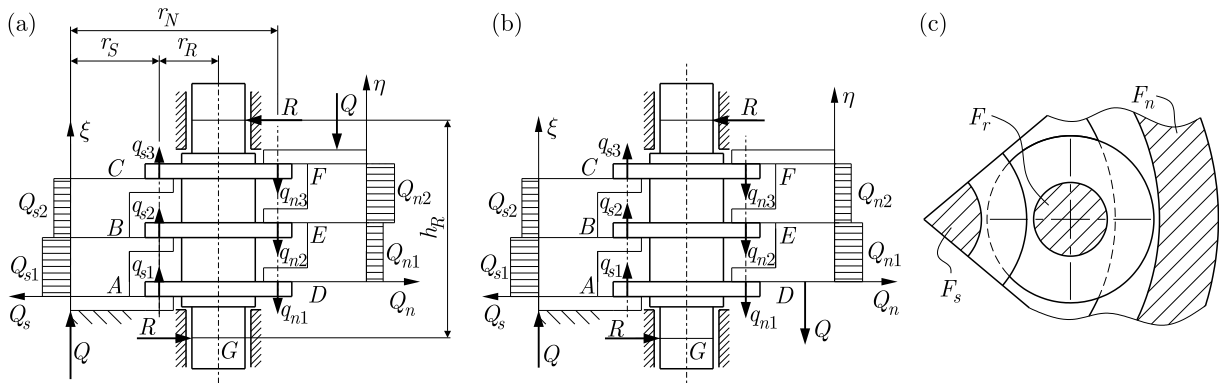


Fig. 2. Dimensions and the system of forces of the bar model: (a) screw and nut compressed, (b) screw compressed, nut tensioned, (c) cross-sections of cooperating elements

considerations, the cases of consistent and opposite loads in the screw and in the nut (Fig. 2a,b) will be considered as an example.

Under the load Q , the cores of the screw and the nut undergo axial displacements Δ_{si} and Δ_{ni} . At the same time, the thread displacements occur: δ_{sj} at the screw-roller thread interface and δ_{nj} at the nut-roller threads interface. These displacements include contact deformations as well as shear strains. The displacements of cooperating elements and dimensional chains are shown in Fig. 3.

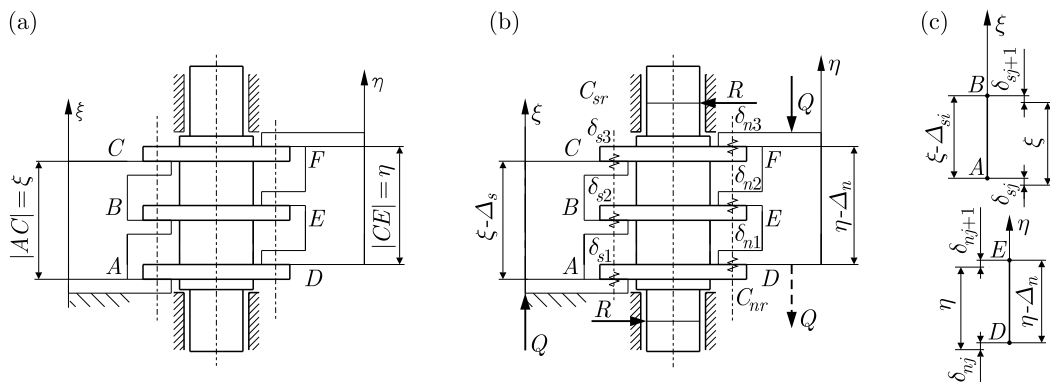


Fig. 3. Deformations of planetary roller screw elements: (a) unloaded model, (b) loaded model, (c) dimensional chains

According to Hooke's law, assuming that stress in cross-sections of the screw and nut cores is distributed uniformly, the axial displacements of the screw core for any value of $\xi < |AC|$ and, respectively, the axial displacement of the nut core for any value of $\eta < |DF|$ are obtained from the following equation

$$\Delta_s = \int_0^{\xi_a} \frac{\sigma_s(\xi)}{E_s} d\xi = \int_0^{\xi_a} \frac{Q_s(\xi)}{E_s F_s} d\xi \quad \Delta_n = \int_0^{\eta_a} \frac{\sigma_n(\eta)}{E_n} d\eta = \int_0^{\eta_a} \frac{Q_n(\eta)}{E_n F_n} d\eta \quad (2.1)$$

where $\sigma_s(\xi)$, $\sigma_n(\eta)$ are normal stresses in cross-sections of the screw and nut cores; $Q_s(\xi)$, $Q_n(\eta)$ – axial forces in the screw and in the nut; E_s , E_n – Young's modules of the screw and the nut; F_s , F_n – cross-sectional areas of the screw and nut cores.

Assuming a step change of forces in cross-sections of the screw and nut cores (wherein the step is equal to the thread pitch) and accepting n intervals of force variation, Eq. (2.1) takes the form

$$\Delta_s = \sum_{i=1}^n \Delta_{s_i} = \sum_{i=1}^n \frac{Q_{s_i} p}{E_s F_s} \quad \Delta_n = \sum_{i=1}^n \Delta_{n_i} = \sum_{i=1}^n \frac{Q_{n_i} p}{E_n F_n} \quad (2.2)$$

where Δ_{s_i} , Δ_{n_i} are axial displacements of cross-sections of the screw and nut cores; Q_{s_i} , Q_{n_i} – axial forces in the screw and in the nut for the i -th interval ($i = 1, \dots, n$, n – number of intervals of force variation); p – thread pitch.

Axial displacements at the interfaces of the screw-roller and roller-nut threads, which include contact deformations as well as shear strains, can be determined as

$$\delta_{s_j} = \frac{q_{s_j}}{C_{sr}} \quad \delta_{n_j} = \frac{q_{n_j}}{C_{nr}} \quad (2.3)$$

where C_{sr} , C_{nr} are stiffness coefficients of the screw-roller and the roller-nut cooperation; q_{s_i} , q_{n_i} – axial forces at the interfaces of the screw-roller and the roller-nut threads ($j = 1, \dots, m$, m – number of threads). Considering the system of forces shown in Fig. 2a, the axial forces in the screw and in the nut in the case of consistent loads can be determined using Eqs. (2.4). Consequently, for the opposite loads in the screw and in the nut (Fig. 2b), Eqs. (2.5) can be used. The axial load is a sum of forces on threads as given by Eqs. (2.6)

$$\begin{cases} Q_{s_1} = Q - q_{s_1} \\ Q_{s_2} = Q - q_{s_1} - q_{s_2} \end{cases} \quad \begin{cases} Q_{n_1} = Q - q_{n_3} - q_{n_2} \\ Q_{n_2} = Q - q_{n_3} \end{cases} \quad (2.4)$$

$$\begin{cases} Q_{s_1} = Q - q_{s_1} \\ Q_{s_2} = Q - q_{s_1} - q_{s_2} \end{cases} \quad \begin{cases} Q_{n_1} = Q - q_{n_1} \\ Q_{n_2} = Q - q_{n_1} - q_{n_2} \end{cases} \quad (2.5)$$

$$Q = q_{s_1} + q_{s_2} + q_{s_3} \quad Q = q_{n_1} + q_{n_2} + q_{n_3} \quad (2.6)$$

Considering the dimensional chains obtained for the loaded model (Fig. 3b,c), the displacement equilibrium equations take the following form

$$\begin{aligned} \Delta_{S1} &= \delta_{S1} - \delta_{S2} & \Delta_{N1} &= \delta_{N2} - \delta_{N1} \\ \Delta_{S2} &= \delta_{S2} - \delta_{S3} & \Delta_{N2} &= \delta_{N3} - \delta_{N2} \end{aligned} \quad (2.7)$$

Taking into account Eqs. (2.2)-(2.7), the system of equations for determination of the load distribution are obtained. Equations (2.8) refer to the case of the consistent load in the screw and the nut while Eqs. (2.9) refer to the case of the opposite load in the screw and the nut. In both cases, the sum of loads on threads is equal to the axial load as given by Eq. (2.10)

$$\frac{p}{E_s F_s} \left(Q - \sum_{j=1}^i q_{s_j} \right) = (C_{sr})^{-1} (q_{s_i} - q_{s_{i+1}}) \quad (n \text{ equations}) \quad (2.8)$$

$$\frac{p}{E_n F_n} \left(Q - \sum_{j=i+1}^m q_{n_j} \right) = (C_{nr})^{-1} (q_{n_i} - q_{n_{i+1}}) \quad (n \text{ equations})$$

$$\frac{p}{E_s F_s} \left(Q - \sum_{j=1}^i q_{s_j} \right) = (C_{sr})^{-1} (q_{s_i} - q_{s_{i+1}}) \quad (n \text{ equations}) \quad (2.9)$$

$$\frac{p}{E_n F_n} \left(Q - \sum_{j=1}^i q_{n_j} \right) = (C_{nr})^{-1} (q_{n_{i+1}} + q_{n_i}) \quad (n \text{ equations})$$

$$Q = \sum_{j=1}^m q_{s_j} \quad Q = \sum_{j=1}^m q_{n_j} \quad (2.10)$$

$j = 1, \dots, m$, m – number of threads; $i = 1, \dots, n$, n – number of intervals of force variation.

2.1. Determination of the stiffness coefficients

Stiffness coefficients of the screw-roller thread pair (C_{sr}) as well as the nut-roller thread pair (C_{nr}) can be determined using FE analysis. The finite element models including sections of cooperating pairs of threads and the accepted boundary conditions are shown in Fig. 4. A triangular thread profile with the pressure angle $\alpha_0 = 45^\circ$ has been accepted. The helix angle has been omitted.

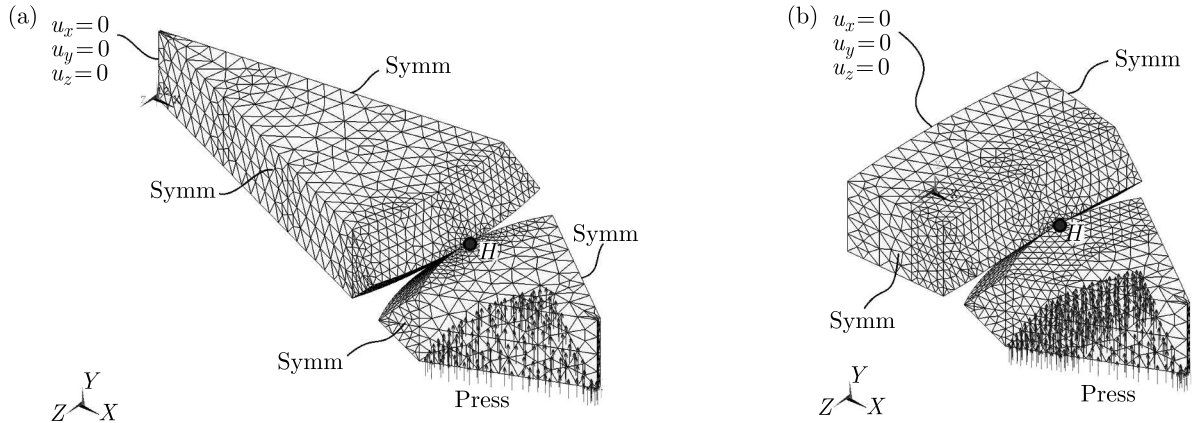


Fig. 4. Finite element models of the screw-roller, nut-roller sections with boundary conditions

The load is applied to the roller core as a normal pressure. The axial displacement u_y is measured in the point H . The stiffness coefficients are determined using the following equations

$$C_{sr} = \frac{P_H}{u_y} \quad C_{nr} = \frac{P_H}{u_y} \quad P_H = \frac{P_n x_c}{r_r - h_z/2} \quad (2.11)$$

where P_n is the normal load on the roller core surface (axial load per single pair of cooperating threads), P_H – normal load on the roller core surface reduced to the point H , x_c – distance between the gravity centre of the roller core cross-section and the roller axis, h_z – height of the thread profile, r_r – pitch diameter of the roller.

Stiffness coefficients for various load levels and for a series of pitch diameter combinations referred to the triangular thread profile, can also be assumed using the graphs presented by Lisowski (2015).

2.2. Load distribution based on the bar model

Examples of theoretical load distributions obtained for the bar model are shown in Figs. 5a and 5b. The accepted parameters of the planetary roller screw and load conditions are presented in Table 1. The stiffness coefficients of the screw-roller thread pair and the nut-roller thread pair have been determined as has been stated in the previous Section.

3. Specific dynamic capacity of the planetary roller screw

Taking into account a formula for the rolling contact life, the specific dynamic capacity of the planetary roller screw depends on the equivalent load transferred by the mechanism, as given by

$$N = \left(\frac{C}{P}\right)^3 N_0 \quad (3.1)$$

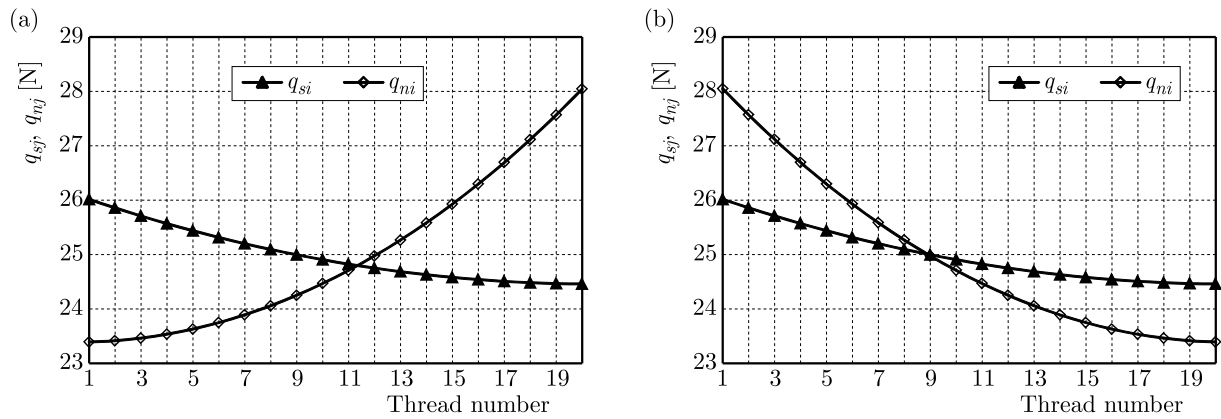


Fig. 5. Load distribution on the screw (q_{si}) and nut (q_{ni}) threads – (a) consistent and (b) opposite loads in the screw and the nut; $r_s = 15$ mm, $r_r = 5$ mm, $r_n = 25$ mm, $p = 2$ mm, $m = 5$, $P_n = 25$ N

Table 1. Planetary roller screw parameters

Pitch radius of screw	$r_s = 15$ mm
Pitch radius of roller	$r_r = 5$ mm
Pitch radius of nut	$r_n = 25$ mm
Lead	$p = 2$ mm
Pressure angle	$\alpha_0 = 45^\circ$
Number of intervals of force variation	$n = 19$
Number of threads	$m = 20$
Axial load per one roller	$Q = 500$ N
Axial load per single pair of cooperating threads	$P_n = 25$ N
Stiffness coefficient of screw-roller thread pair	$C_{sr} = 2505$ N/mm
Stiffness coefficient of nut-roller thread pair	$C_{nr} = 7482$ N/mm

where N is life in million cycles, N_0 – life equal to 1 million cycles, C – specific dynamic capacity, P – equivalent load. According to Lisowski (2015), limitation of the planetary roller screw capacity is related to the permissible contact pressure between threads of the screw and the roller. Therefore, the analysis of PRS capacity is referred to cooperation of the screw and the roller. Considering the screw-roller cooperation, the equivalent load can be accepted as the average load on all threads.

However, the actual dimensions of threads would be subjected to random deviations. Distributions of the deviations are very diverse and usually have an irregular form. They can be determined based on the results of measurements of a large batch of machined parts under stated conditions, for example by building a histogram of deviations. However, in many cases, a theoretical distribution determined empirically can be accepted. Referring to (Białas, 1986), if many independent factors affect manufacturing deviations, the normal distribution, defined by the density function of deviations, is obtained.

Taking into account the random deviations of the thread pitch, the load density distribution related to the average load of threads ($x = P_i/P_{ave}$) is a normal distribution given by

$$\psi(x) = \frac{1}{\sigma\sqrt{2\pi}} \exp\left(-\frac{(x-\mu)^2}{2\sigma^2}\right) \quad (3.2)$$

where σ is the standard deviation, μ – expected value.

Assuming that the PRS life $N = N_0 = 1$ million cycles, the specific dynamic capacity is proportional to the equivalent load. Consequently, the same relation is obtained when the random deviations of the thread pitch are taken into account

$$C = P \quad C_{dev} = P_{dev} \tag{3.3}$$

Since in Eq. (3.1) the relation between the specific dynamic capacity and the equivalent force is to the third power, the function given by Eq. (3.4)₁ is accepted. The integral of this function, which can be expressed as a sum, is given by Eq. (3.4)₂

$$\eta(x) = [\psi(x)]^3 \quad \eta_1 = \int_0^x [\psi(x)]^3 dx = \frac{1}{n_i} \sum \left(\frac{P_i}{P_{ave}} \right)^3 \quad n_i = n_t + n_d \tag{3.4}$$

where P_i are axial forces on particular threads in the case with random deviations of the thread pitch, P_{ave} – average load of all threads, n_i – number of forces including the number of cooperating threads and the number of intervals of deviation variation, n_t – number of cooperating threads, n_d – number of intervals of deviation variation.

The equivalent force as well as the specific dynamic capacity, including random deviations of the thread pitch, can be determined using Eqs. (3.5)_{1,2}. The decrease of the specific dynamic capacity caused by the occurrence of random deviations can be estimated as

$$P_{dev} = P_{ave} \sqrt[3]{\frac{1}{n_i} \sum \left(\frac{P_i}{P_{ave}} \right)^3} \quad C_{dev} = C \sqrt[3]{\frac{1}{n_i} \sum \left(\frac{P_i}{P_{ave}} \right)^3} \tag{3.5}$$

$$\Delta_{dev} = \left| \frac{C_{dev}}{C} - 1 \right|$$

where P_{dev} is the equivalent load including random deviations of the thread pitch C – specific dynamic capacity of PRS excluding random deviations of the thread pitch, C_{dev} – specific dynamic capacity including random deviations of the thread pitch, Δ_{dev} – decrease of the specific dynamic capacity caused by the random deviations of the thread pitch.

3.1. The impact of random deviations of the thread pitch on the decrease of the specific dynamic capacity of PRS

A series of calculations using the bar model to determine the load distribution has been conducted in order to obtain load distributions including random deviations of the thread pitch. Those load distributions are analysed to assess how the magnitude of random deviations of the thread pitch affects the specific dynamic capacity of the planetary roller screw. The load case, in which the screw is compressed, is considered. In that case, the load distribution between the screw and the roller, including random deviations of the thread pitch, can be obtained by introducing an additional displacement δ_i^{sr} into Eq. (2.8)₁. This displacement represents the value of the random deviation of the thread pitch. As a result, a system of equations Eq. (3.6)₁ is obtained, wherein the sum of loads on particular threads is equal to the axial load as given by Eq. (3.6)₂

$$\frac{p}{E_s F_1} \left(Q - \sum_{j=1}^i qS_j \right) + \delta_i^{sr} = (C_{S-R})^{-1} (qS_i - qS_{i+1}) \quad (n \text{ equations}) \tag{3.6}$$

$$Q = \sum_{j=1}^m qS_j$$

$j = 1, \dots, m$, m – number of threads; $i = 1, \dots, n$, n – number of intervals of force variation.

One thousand load distributions including random deviations of the thread pitch has been assumed for the particular case of analysis. The random deviations have been generated using a random number generator implemented in MATLAB. For each pair of cooperating threads of the screw and the roller, one thousand random deviations has been generated. Due to the lack

of information about results of measurements of a large batch of machined PRS parts under the stated conditions, the probability density function of normal (Gaussian) distribution with a mean of $\mu = 0$ and standard deviation $\sigma = 2$ has been assumed (Fig. 6). The random deviations in μm generated for the desired parameters of normal distribution are presented in Table 2 and as a surface graph in Fig. 7.

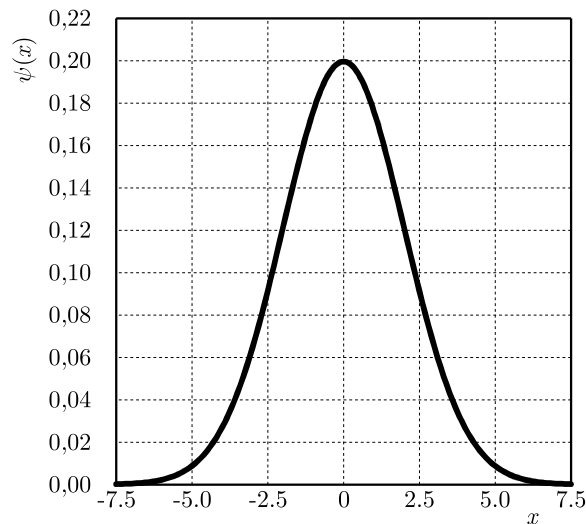


Fig. 6. Gaussian density distribution of random deviations ($\mu = 0$, $\sigma = 2$)

Table 2. Random deviations in μm ($\mu = 0$, $\sigma = 2$)

		Thread number											
		1	2	3	4	5	6	7	8	9	10	...	20
Sampling number	1	2.611	-0.855	-0.983	-2.884	-1.291	-2.100	-3.837	-0.277	2.282	0.328	2.221	2.221
	2	1.968	-1.159	1.315	-1.920	-0.578	0.937	-0.262	0.864	1.866	-1.414	...	1.427
	3	-2.503	1.852	2.872	0.695	2.001	0.566	-1.537	4.506	-1.041	4.593	...	-1.292
	4	-0.360	0.011	-3.070	-0.206	-1.176	2.682	4.780	-0.919	-1.179	0.855	...	1.753
	5	-1.487	-1.269	3.506	1.321	3.115	0.761	0.154	0.181	2.763	3.224	...	0.171
	6	0.466	1.717	2.566	2.314	-2.723	2.871	0.751	5.216	-0.609	-1.302	...	-0.121
	7	4.203	-0.962	0.187	-1.839	3.800	1.599	0.791	-2.074	0.391	-1.907	...	-0.790
	8	-1.753	2.979	3.160	-1.941	0.356	3.257	-0.225	0.506	2.318	-2.077	...	-2.759
	9	3.898	-1.259	0.490	0.912	-4.333	0.258	-3.658	-0.533	0.066	1.107	...	-1.033
	10	-0.931	-1.188	-2.041	-0.242	1.414	-4.170	4.183	2.635	-1.910	0.974	...	-1.021

1000	2.706	-0.844	0.652	-2.440	-2.416	0.206	-2.889	-2.219	-0.382	0.445	...	3.456	

In order to assess the impact of magnitude of the random deviations of the thread pitch on the decrease of the specific dynamic capacity of PRS, the decreasing coefficient f , defined by Eq. (3.7), has been accepted. This coefficient refers to the average axial displacement of all threads in the case without random deviations of the thread pitch. Therefore, the impact of the load level is included as

$$f = \frac{\kappa_{dev} u_0}{\delta_{max}} \quad (3.7)$$

where δ_{max} is the maximum value of random deviations, u_0 – average axial displacement of all threads in the case without random deviations of the thread pitch, κ_{dev} – factor determining the relation between the maximum random deviation δ_{max} and the average axial displacement u_0 , wherein $\kappa_{dev} = \{10, 20, 40\}\%$.

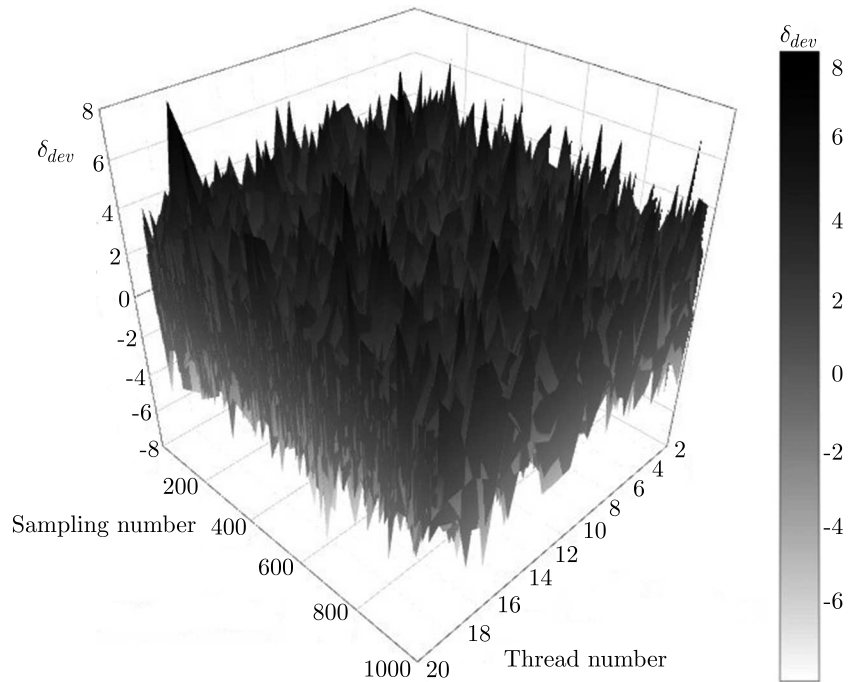


Fig. 7. Surface plot of 20 000 random deviations of the thread pitch

For the considered geometry of PRS, the average axial displacement of all threads in the case without random deviations of the thread pitch is $u_0 = 19.973 \mu\text{m}$. The maximum drawn deviation, obtained among 20 000 values, is $\delta_{max} = 8.184$. Accordingly, the decreasing coefficients, listed in Table 3, have been accepted.

Table 3. Decreasing coefficients and maximum random deviations

κ_{dev}	f	$\delta_{max} [\mu\text{m}]$
10%	0.244	1.997
20%	0.488	3.977
40%	0.976	7.990

Tables of random deviations for three considered values of κ_{dev} have been obtained by multiplying the values of random deviations in Table 2 by the consecutive f coefficients. Table 4, referring to the case of $\kappa_{dev} = 10\%$, presents exemplary results. In the same case, one thousand load distributions between the screw and the roller including random deviations of thread pitch are presented in a surface plot in Fig. 8.

Using Eq. (3.5)₃, the decrease of the specific dynamic capacity related to particular threads and to all cooperating threads of the screw and the roller have been determined. The results of calculations are presented in Figs. 9a and 9b.

4. Conclusions

The decrease of the specific dynamic capacity related to particular threads is the greatest in the end parts of the roller. The largest decrease occurs on the first engaged threads, which are in fact the most loaded ones. Concerning the cooperation of all engaged threads, it has been shown that the decrease of the specific dynamic capacity increases with an increase in the random deviations of the thread pitch. In the case in which the maximum deviation of the thread pitch

Table 4. Random deviations in μm ($\mu = 0, \sigma = 2$); $\kappa_{dev} = 10\%$, $f = 0.244$

		Thread number											
		1	2	3	4	5	6	7	8	9	10	...	20
Sampling number	1	0.637	-0.209	-0.240	-0.704	-0.315	-0.512	-0.936	-0.068	0.557	0.080	0.542	0.542
	2	0.480	-0.283	0.321	-0.469	-0.141	0.229	-0.064	0.211	0.455	-0.345	...	0.348
	3	-0.611	0.452	0.701	0.170	0.488	0.138	-0.375	1.099	-0.254	1.121	...	-0.315
	4	-0.088	0.003	-0.749	-0.050	-0.287	0.655	1.166	-0.224	-0.288	0.209	...	0.428
	5	-0.363	-0.310	0.855	0.322	0.760	0.186	0.038	0.044	0.674	0.787	...	0.042
	6	0.114	0.419	0.626	0.565	-0.664	0.700	0.183	1.273	-0.149	-0.318	...	-0.030
	7	1.025	-0.235	0.046	-0.449	0.927	0.390	0.193	-0.506	0.095	-0.465	...	-0.193
	8	-0.428	0.727	0.771	-0.474	0.087	0.795	-0.055	0.124	0.566	-0.507	...	-0.673
	9	0.951	-0.307	0.119	0.223	-1.057	0.063	-0.893	-0.130	0.016	0.270	...	-0.252
	10	-0.227	-0.290	-0.498	-0.059	0.345	-1.017	1.021	0.643	-0.466	0.238	...	-0.249

1000	0.660	-0.206	0.159	-0.595	-0.589	0.050	-0.705	-0.541	-0.093	0.109	...	0.843	

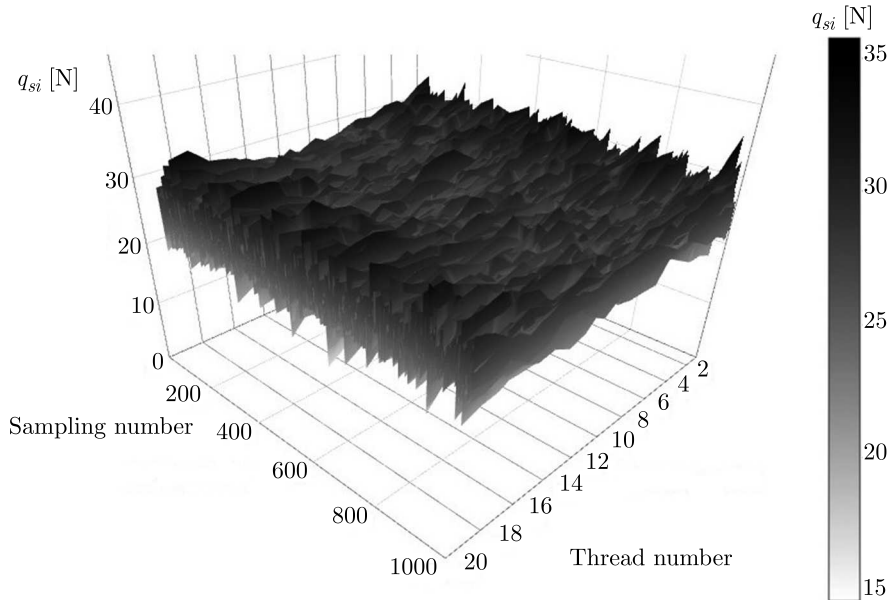


Fig. 8. Surface plot of one thousand load distributions between the screw and the roller including random deviations of the thread pitch ($f = 0.244, \kappa_{dev} = 10\%$)

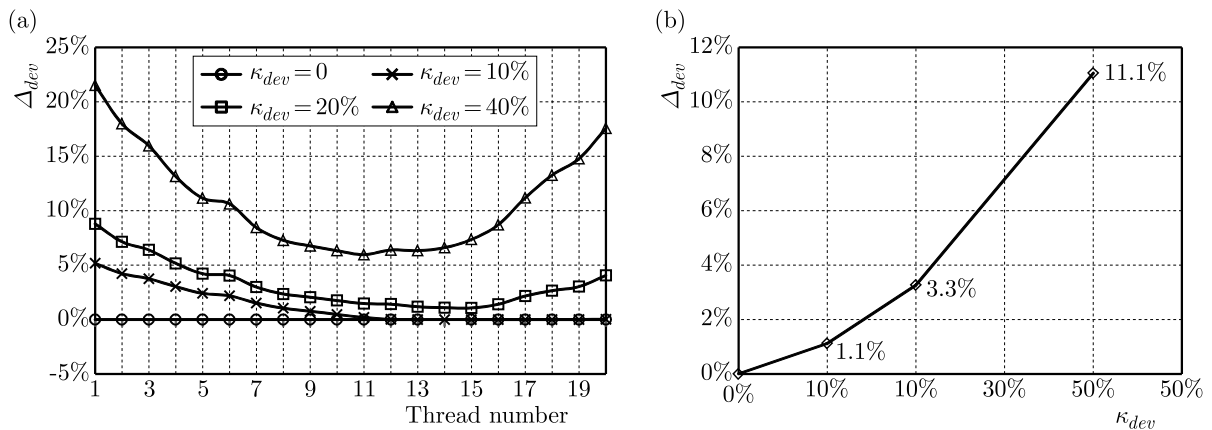


Fig. 9. Decrease of the specific dynamic capacity for: (a) particular screw-roller threads pair, (b) all cooperating threads

does not exceed 20% of the average axial displacement of all the threads, the maximum decrease in the specific dynamic capacity of PRS is small and equals 3.3%. On the other hand, in the case where the maximum deviation of the thread pitch is 40% of the average axial displacement of all the threads, the decrease of the specific dynamic capacity is up to 11.1%. Based on the analysis, it can be concluded that the maximum deviation of the thread pitch, which does not significantly affect the reduction of the specific dynamic capacity of the planetary roller screw under the nominal load, should not exceed 20% of the average axial displacement of all the threads.

Similar results can be expected for different dimensions of the planetary roller screw. This is due to taking into account the relation between the random deviations of the thread pitch and the average displacement of all the threads for the accepted load level.

While considering the essence of cooperation of the PRS elements, we deal with a multipoint support. Therefore, the specific dynamic capacity does not depend on the capacity of the most loaded pair of threads. Even if the carrying capacity of this pair is exhausted, the other threads take over the load. The specific dynamic capacity of a significant number of thread pairs has to be exhausted, to exhaust the carrying capacity of the planetary rollers screw.

Accordingly, the decrease of the specific dynamic capacity of all the cooperating threads, presented in Fig. 9b, is the conclusive parameter.

A similar procedure of assessing the impact of random deviations of the thread pitch on the specific dynamic capacity can be also carried out in the case of non-Gaussian distributions of random deviations.

References

1. ABEVI F.K., DAIDIÉ A., CHAUSSUMIER M., SARTOR M., 2015, Static load distribution and axial stiffness in a planetary roller screw mechanism, *Journal of Mechanical Design*, doi: 10.1115/1.4031859
2. BIAŁAS S., 1986, *Tolerancje geometryczne*, PWN, Warszawa
3. JONES M.H., VELINSKY A., 2014, Stiffness of the roller screw mechanism by the direct method, *Mechanics Based Design of Structures and Machines: An International Journal*, **42**, 17-34, doi: 10.1080/15397734.2013.839385
4. LISOWSKI F., 2014, The Analysis of displacements and the load distribution between elements in a Planetary Roller Screw, *Applied Mechanics and Materials*, **680**, 361-364
5. LISOWSKI F., 2015, *Load analysis and optimization design of selected planetary roller screws* (in Polish), Wydawnictwo Politechniki Krakowskiej, ISBN 978-83-7242-865-3
6. MA S., LIU G., TONG R., ZHANG X., 2012, A new study on the parameter relationships of planetary roller screws, *Mathematical Problems in Engineering*, Article ID 340437, doi: 10.1155/2012/340437
7. MEI X., TSUTSUMI M., TAO T., SUN N., 2003, Study on the load distribution of ball screws with errors, *Mechanism and Machine Theory*, **38**, 1257-1269
8. RYŚ J., 1990, Transient and steady vibration of helical gears, *Journal of Theoretical and Applied Mechanics*, **28**, 1/2, 207-216
9. RYŚ J., LISOWSKI F., 2014, The computational model of the load distribution between elements in planetary roller screw, *Journal of Theoretical and Applied Mechanics*, **52**, 3, 699-705
10. VELINSKY A., CHU B., LASKY T.A., 2009, Kinematics and efficiency analysis of the planetary roller screw mechanism, *Journal of Mechanical Design*, **131**, doi: 10.1115/1.3042158.